

RESEARCH

Open Access



Deciphering the molecular nexus of BTG2 in periodontitis and diabetic kidney disease

Binhui Pan^{1†}, Yangyang Teng^{2†}, Renban Wang¹, Dan Chen¹ and Hui Chen^{1*}

Abstract

Objective To investigate the role of *BTG2* in periodontitis and diabetic kidney disease (DKD) and its potential underlying mechanism.

Methods Gene expression data for periodontitis and DKD were acquired from the Gene Expression Omnibus (GEO) database. Differential expression analysis identified co-expressed genes between these conditions. The Nephroseq V5 online nephropathy database validated the role of these genes in DKD. Pearson correlation analysis identified genes associated with our target gene. We employed Gene Set Enrichment Analysis (GSEA) and Protein-Protein Interaction (PPI) networks to elucidate potential mechanisms. Expression levels of *BTG2* mRNA were examined using quantitative polymerase Chain Reaction (qPCR) and immunofluorescence assays. Western blotting quantified proteins involved in epithelial-to-mesenchymal transition (EMT), apoptosis, mTORC1 signaling, and autophagy. Additionally, wound healing and flow cytometric apoptosis assays evaluated podocyte migration and apoptosis, respectively.

Results Analysis of GEO database data revealed *BTG2* as a commonly differentially expressed gene in both DKD and periodontitis. *BTG2* expression was reduced in DKD compared to normal conditions and correlated with proteinuria. GSEA indicated enrichment of *BTG2* in the EMT and mTORC1 signaling pathways. The PPI network highlighted *BTG2*'s relevance to *S100A9*, *S100A12*, and *FPR1*. Immunofluorescence assays demonstrated significantly lower *BTG2* expression in podocytes under high glucose (HG) conditions. Reduced *BTG2* expression in HG-treated podocytes led to increased levels of EMT markers (α -SMA, vimentin) and the apoptotic protein Bim, alongside a decrease in nephrin. Lower *BTG2* levels were associated with increased podocyte mobility and apoptosis, as well as elevated RPS6KB1 and mTOR levels, but reduced autophagy marker LC3.

Conclusion Our findings suggest that *BTG2* is a crucial intermediary gene linking DKD and periodontitis. Modulating autophagy via inhibition of the mTORC1 signaling pathway, and consequently suppressing EMT, may be pivotal in the interplay between periodontitis and DKD.

Keywords Diabetic kidney disease, Periodontitis, Bioinformatics analysis, EMT, Autophagy

[†]Binhui Pan and Yangyang Teng contributed equally to this work and share first authorship.

*Correspondence:

Hui Chen

dadahui0302@126.com

¹Department of Nephrology, Wenzhou Central Hospital, Wenzhou, Zhejiang Province, China

²Department of Gastroenterology, The Second Affiliated Hospital, Yuying Children's Hospital of Wenzhou Medical University, Wenzhou, Zhejiang Province, China



Introduction

Diabetic Kidney Disease (DKD), a prevalent complication of diabetic microangiopathy, stands as a primary cause of Chronic Kidney Disease (CKD). Notably, about 40% of individuals with type 2 diabetes and 30% of those with type 1 diabetes eventually develop kidney-related complications [1, 2]. Many patients progress to end-stage renal disease (ESRD) by the time of diagnosis. Therefore, elucidating the underlying mechanisms of DKD is crucial for early detection and intervention, significantly impacting the disease's progression.

Periodontitis used to be considered to primarily affect oral and dental health, often resulting in tooth loss. Recently years, periodontitis has been linked to a range of systemic diseases [3–7]. Notably, in a 22-year follow-up study of type 2 diabetes patients conducted by Shultis et al. in 2007, the incidence of proteinuria and ESRD was found to increase with the severity of periodontitis. Patients with moderate to severe periodontitis, or those who were edentulous, exhibited a 2.3 to 4.9-fold higher incidence of ESRD compared to those with no or mild periodontitis [8]. Further studies have established a connection between oral pathogenic bacteria and DKD [9, 10].

However, the mechanisms linking periodontitis and DKD remain largely unexplored. In this study, we employed bioinformatics techniques and cellular functional assays to identify key interacting genes between periodontitis and DKD. The results indicated that *BTG2* was the essential crosstalk gene between these two diseases. *BTG2*, part of the *BTG/Tob* family, regulates the cell cycle and various cellular activities [11]. As the first protein identified in *BTG/Tob* family, *BTG2* possesses the ability to promote programmed cell death or survival [12]. Initially studied as an antioncogene [13–16], recent research has linked *BTG2* to non-tumor conditions, including retinal microvascular endothelial cell proliferation [17], impaired blood pressure control and proteinuria [18], suggesting its potential importance in DKD. In our study, we demonstrated the decline of *BTG2* in DKD and investigated the potential underlying cellular and molecular mechanisms, aiming to provide novel insights for the prevention and treatment of DKD.

Methods

Datasets download

Gene expression datasets for periodontitis and diabetic kidney disease (DKD) were obtained from the Gene Expression Omnibus (GEO) database (<https://www.ncbi.nlm.nih.gov/geo/>). The GSE16134 dataset, based on GPL570-55599, included 310 gingival papillae samples from 120 subjects undergoing periodontal surgery, comprising 241 “diseased” and 69 “healthy” samples. GSE10334, also based on GPL570-55599, contained 247

gingival papillae samples from 90 periodontitis patients, with 183 “diseased” and 64 “healthy” samples. For DKD, the GSE96804 dataset was based on the GPL17586 platform, including 61 samples (41 from DKD patient glomeruli and 20 from normal glomeruli from tumor nephrectomy).

Mutual differentially expressed genes identification and correlation analysis

Differential expression analysis was set with a threshold of \log_2 Fold Change (FC) >1 or <-1 and an adjusted P-value <0.05, using the “limma” package in R software. The Nephroseq V5 online nephropathy database (<https://www.nephroseq.org/>) was used for analyzing related gene expression between DKD and normal conditions, and for clinical correlation analysis of differentially expressed genes (DEGs). DEG correlation analysis was conducted on the DKD dataset GSE96804. A correlation coefficient threshold of >0.5 or <-0.5 and a P-value <0.05 were used for Pearson correlation analysis. Differential analysis employed the limma package in R software with \log_2 FC thresholds of >1.5 or <-1.5 and an adjusted P-value <0.05.

Pathway enrichment analysis and protein-protein interaction networks

DEGs between high and low expression groups, based on the target DEG expression level in GSE96804, were identified. Gene Set Enrichment Analysis (GSEA) was carried out through gene sets *h.all.v7.1.symbols.gmt* and *c2.cp.kegg.v7.1.symbols.gmt*, respectively. The related genes were screened in the STRING database, and the Protein-Protein Interaction (PPI) networks were constructed using software Cytoscape, and core gene groups were filtered by Molecular Complex Detection (MCODE).

Antibodies and cell culture

Mouse kidney foot cells (MPC5) were purchased from Shanghai iCell Bioscience Inc (Shanghai, China) and were cultured in dulbecco's modified eagle medium (DMEM) supplemented with 10% high quality fetal bovine serum in the humidified incubator at 37°C 5% CO₂. Rabbit anti-*BTG2* antibody (bs-0031R) was purchased from Beijing Bioss Biotechnology Co., Ltd while α -SMA, vimentin, Bim, pMTOR, MTOR, RPS6KB1, LC3 antibodies and nephrin, pRPS6KB1 antibodies were purchased from Wuhan Proteintech Group, Inc and Jiangsu Affinity Biosciences Ltd, respectively. Detailed procedures are described in the Supplementary Materials.

Gene knockdown/overexpression cell lines establishment

Lentivirus-packaged *BTG2*-targeting siRNA was used to *BTG2* knockdown, while lentivirus-packaged *BTG2* plasmid was used to *BTG2* overexpression. MPC5 cells were plated (24-well plate) and cultured in DMEM complete

medium containing 10% FBS for 24 h to ensure a cell confluence of 20–40% and cells were in good condition. Prior to infection, we diluted the infection enhancer solution P in complete culture medium at a ratio of 24:1 and removed the original cell culture medium. After washing the cells with phosphate buffered saline (PBS), we added the medium containing the infection enhancer solution and diluted the virus to a titer of 1×10^8 TU/mL by complete culture medium. Calculating the needed volume of virus according to the MOI value ($\text{MOI} \times \text{number of cells} / \text{virus titer}$), we added 5 μL of virus solution to each well for infection. After 16 h of infection, we replaced the medium with complete culture medium and cultured for an additional 48 h. Approximately 72 h post-viral infection, infection efficiency (cell growth reached 90–100%) was observed. Detailed procedures are described in the Supplementary Materials.

Optimal time point selection for BTG2 downregulation

Quantitative polymerase chain reaction (qPCR) was used to detect the expression of BTG2 in podocytes of each group. Podocytes were planted in six-well plates and divided into normal group (Control group) and HG (30mmol/L) stimulated groups for 12 h, 24 h, 36 h and 48 h. We added 1 ml Trizol to the cells, followed by centrifuge. Then we added 200 μL chloroform to the Trizol solution and then centrifuged. Added an equal volume of isopropanol (300–400 μL), mixed, and held at room temperature for 10 min. After centrifuge we added 1000 μL of 75% ethanol (equal volume to RNAiso Plus), mixed, and centrifuged. Washed and added 20 μL DEPC to dissolve RNA, we took 2 μL for RNA concentration measurement on NanoDrop. The remaining RNA was dissolved in 20 μL DEPC water, then the dissolved RNA was reverse transcribed into cDNA. According to the final measurement, the optimal time point for downregulation of BTG2 stimulated by HG was selected. Detailed procedures are described in the Supplementary Materials.

Immunofluorescence assays

First, we prepared a single-cell suspension. We preparing a six-well plate, seeded a certain number (approximately 5×10^5) of cells, and cultured for 24 h or longer until the cells reach confluence of 70–80%. Then we washed each well three times with PBS, fixed with 4% pre-chilled paraformaldehyde. After discarding PBS, we blocked it with approximately 700 μL of 5% BSA solution at room temperature for 1 h. Sequentially we added diluted rabbit anti-BTG2 antibody (bs-0031R, Bioss antibodies) and then incubated overnight at 4 °C. Next we recovered the primary antibody, added diluted fluorescently labeled secondary anti-rabbit antibody (4413 S, Cell Signaling Technology) and incubated at 37 °C in a water bath for 1.5 h. Finally, we discarded the secondary antibody,

washed with PBS, and sealed the coverslip with mounting medium containing DAPI to quench fluorescence. Under a fluorescence microscope in the correct orientation, pictures were taken. Immunofluorescence assay verified BTG2 expression differences under HG stimulation compared to normal conditions. Detailed procedures are described in the Supplementary Materials.

Western Blotting (WB)

WB detected typical proteins related to epithelial-to-mesenchymal transition (EMT) (nephrin, α -SMA, and vimentin), the apoptotic protein Bim, ribosomal protein S6 kinase B1 (RPS6KB1), mammalian target of rapamycin (mTOR), and autophagy protein LC3, with β -actin as an internal reference control. In experiment, after the culture solution was discarded and cleaned twice with PBS, 100 μL cell lysate was added to each well. After cell lysate was disposed, the protein sample was obtained through cracking and centrifuge, followed by albuminous degeneration. After cleaning the assembled glass plate, we prepared the separation and stacking gel according to the SDS-PAGE gel rapid preparation kit instructions. Next we put the prepared gel into the electrophoresis tank, added the electrophoresis solution and then loading. After the loading was finished, the electrophoresis solution was added for protein electrophoresis. Sequentially, a transmembrane sandwich was made and sealed with a protein-free sealing solution. The membrane was cut according to the required molecular weight, and then incubated with first and second antibody successively, and finally exposed and developed. Detailed procedures are described in the Supplementary Materials.

Cell scratch assay

Cell scratch assay mimics the cells migration during healing in the body, which includes creating a “wound” in a monolayer of cells, capturing images at the beginning and periodically during the procedure of cell migration to close the wound, and finally comparing images for cell migration rates determination. We first used a marker pen to draw horizontal lines evenly on the back of the six-well plate, with approximately 0.5–1 cm apart, crossing through each well. Each well should have at least 5 lines. Then, we added approximately 5×10^5 cells into each well. The next day, we utilized a pipette tip to make vertical scratches perpendicular to the horizontal lines on the back of the plate. After washing the cells with PBS three times, we added serum-free culture medium. We placed the plate in a 37 °C, 5% CO₂ cell culture incubator, stimulating with HG. Finally, we sampled and took photographs at 0 and 24 h. Detailed procedures are described in the Supplementary Materials.

The scratch healing rate $= (\text{0 h scratch area} - \text{24 h scratch area}) / \text{0 h scratch area} \times 100\%$.

Flow cytometry

Flow cytometry further verified the effect of *BTG2* on podocyte apoptosis. Treating the cells with HG for 24 h, we washed the cells twice with PBS, then resuspended the cells at a concentration of 1×10^6 cells/ml in $1 \times$ binding buffer. We then transferred 100 μ l of the solution (1×10^5 cells) to a 5 ml culture tube, and added 5 μ l of FITC Annexin V (51-65874X, BD Pharmingen) and 5 μ l of propidium iodide (51-66211E, BD Pharmingen). And 10X Annexin V binding buffer (51-66121E, BD Pharmingen) was diluted into distilled water to make 1X Annexin V binding buffer working liquid. After eddying the cells and incubating in the dark at room temperature (25 °C) for 15 min, 400 μ l of 1X Annexin V binding buffer was added to each tube and analyzed using a flow cytometer within 1 h. The cross gate was set according to the undyed tube and the single dyed tube, so as to conduct the subsequent data analysis. Detailed procedures are described in the Supplementary Materials.

Statistical analysis

Data from GEO database were processed using R software. Experimental data were statistically analyzed using GraphPad and Microsoft Excel. Pearson correlation analysis in R software was conducted using the “cor.test”, with a correlation coefficient threshold of >0.5 or <-0.5 , while pathway enrichment analysis was conducted using “clusterProfiler”. And differential expression analysis was carried out via the “limma” package. One-way analysis of variance was conducted for multiple group comparisons. Bonferroni correction, the final value of which was false discovery rate (FDR), was conducted for multiple hypotheses test and correction. A p value less than 0.05 was considered statistically significant.

Results

Mutual DEGs analysis in periodontitis and DKD

We downloaded periodontitis and DKD gene expression datasets from GEO database. GSE16134 dataset based on GPL570-55599 and GSE10334 dataset based on GPL570-55599 contain 310 gingival papillae data from 120 subjects undergoing periodontal surgery (241 “diseased” and 69 “healthy”) and 247 gingival papillae data from 90 periodontitis patients (183 “diseased” and 64 “healthy”), respectively. The DKD gene expression dataset (GSE96804) is based on GPL17586 platform, including 61 samples (41 from glomeruli of DKD patients and 20 from normal glomeruli of tumor nephrectomy). The differentially expressed genes in the three datasets through the differential analysis of limma package in R software were showed, and a total of 12 co-expressed DEGs were discovered (Fig. 1a). Although the sample size of DKD dataset was not large enough, principal component analysis (PCA) proved a high quality of this dataset

(Fig. 1b). To show the results more vividly, we drawn a volcano plot for these DEGs (Fig. 1c) and details of DEGs including *BTG2*, *C3*, *IGKV1-17*, *SELL*, *FPRI*, *IGKV1-5*, *MMP7*, *FCGR3B*, *CCL18*, *FOS*, *PPBP* and *HBA2* were also established (Fig. 1d).

Among these DEGs, we found that the expression of *BTG2* in DKD patients was significantly lower than the control. Consistently, we employed Nephroseq V5 online nephropathy database and found a lower expression of *BTG2* in DKD than that in normal, with a statistical significance (Fig. 1e). The clinical correlation analysis also showed that there was a strong correlation between *BTG2* expression and proteinuria, while the *BTG2* expression level was higher, the proteinuria amount was less (Fig. 1f). Therefore, we have reason to believe that *BTG2* is a key interactive gene between periodontitis and DKD

BTG2 correlation analysis

We conducted pearson correlation analysis for *BTG2* from DKD samples, and screened genes with correlation coefficient >0.5 or <-0.5 and a p value less than 0.05. Finally, eighteen pivotal related genes were selected including “*ywhaz*”, “*Cluap1*”, “*PIP4K2C*”, “*SERP1*”, “*XBPI*”, “*EXOC6B*”, “*RSRC1*”, “*VNN1*”, “*LENG1*”, “*ABCA2*”, “*HAAO*”, “*UGT3A1*”, “*PGLYRP1*”, “*BTBD18*”, “*KCNH3*”, “*SIX5*”, “*TRAJ59*”, and “*FAM187B*” (Fig. 2).

DEGs screened by *BTG2*

To explore the role of *BTG2* in DKD patients, we divided the DKD samples into high and low expression groups according to the *BTG2* expression level. And in the high expression group, *BTG2* expression level was significantly higher than that in the low, with a high quality of PCA (Fig. 3a and b). Thus, we set the threshold of differential analysis as $\log_2 FC > 1.5$ or <-1.5 and adjust P value <0.05 , sequentially screened out 27 coding genes, and conclusively, summarized to a heat map (Fig. 3c). Correlation analysis between *BTG2* and these coding genes were also conducted (Fig. 3d and e).

DEGs functional analysis

To further analyze the related function of DEGs, we drawn bubble diagram utilizing the gene sets h.all.v7.1.symbols.gmt and c2.cp.kegg.v7.1.symbols.gmt (Fig. 4a/b). Since the former summarized and represented specific well-defined biological states or processes and displayed coherent expression, we further utilized this gene set for pathway enrichment analysis and finally a total of 29 related DEGs enriched pathways were screened. As the figure displayed (Fig. 4c), each bar represents a gene, and the sequence of genes was ordered according to the $\log_2 FC$ of all these genes. However, only the genes enriched in special function would

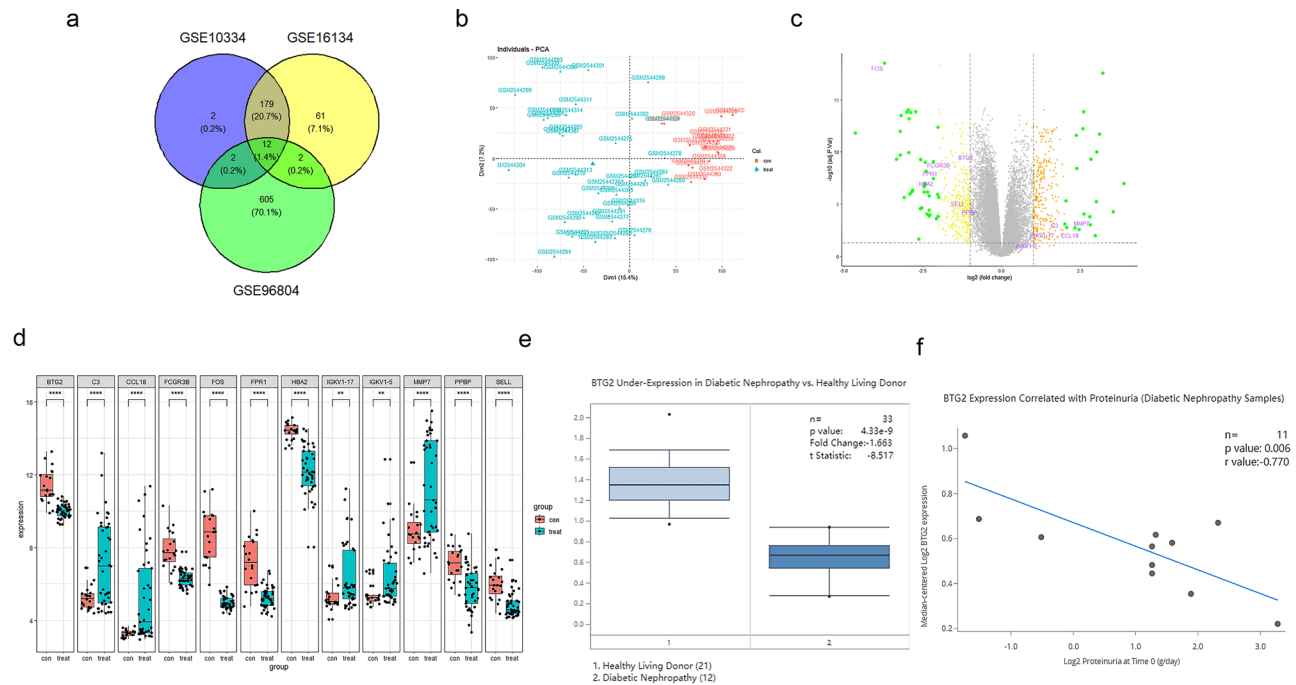


Fig. 1 Mutual DEGs between periodontitis and DKD **(a)** Venn diagram of mutual DEGs between periodontitis (GSE16134, GSE10334) and DKD from GEO (GSE96804) database. There were a total of 12 co-expressed DEGs screened. **(b)** PCA analysis of DKD. Clustered samples indicated little difference between the samples. **(c)** Volcano plot of DEGs. \log_2 FC > 1 or < -1, an adjusted P-value < 0.05. **(d)** Histogram of DEGs. Compared to the control, *BTG2*, *FPR1*, *FCGR3B*, *FOS*, *HBA2*, *SELL*, *PPBP* were decreased, and *C3*, *IGKV1-17*, *IGKV1-5*, *MMP7* and *CCL18* were increased. **(e)** *BTG2* expression in diabetic kidney and healthy living donor from Nephroseq V5 online nephropathy database. Compared to the normal, *BTG2* expression in DKD was significantly decreased. **(f)** The correlation between *BTG2* expression and proteinuria. With higher *BTG2* expression level, DKD patients have less proteinuria. $P < 0.05$ has a statistical significance. **, $P < 0.01$; ***, $P < 0.001$; ****, $P < 0.0001$

be displayed. The vertical coordinates represented the enrichment scores of the genes. Positive scores could be regarded as gene activation, and negative scores could be regarded as gene inhibition. The results showed that DEGs were enriched in EMT pathway and mTORC1 signal pathway, suggesting that *BTG2* might affect DKD prognosis through EMT and mTORC1 pathway.

Then, we gathered the above 18 highest correlated genes and the 27 DEGs in the STRING database, constructed PPI network by cytoscape software (Fig. 4d). Ultimately, we screened out three core gene groups by MCODE, among which the *BTG2* located in proving that *BTG2* was relevant to *S100A9*, *S100A12*, *FPR1* and some other genes.

Cellular functional assays

In order to test our hypothesis, we performed cellular functional assays. First, we used qPCR observe the *BTG2* mRNA expression level under different HG exposure time (Fig. 5a). We found that 24 h-HG exposure lead to a lowest BTG expression level, so 24 h was set as the optimal exposure time. Immunofluorescence assay showed that compared with normal podocytes, the expression level of *BTG2* in podocytes dealt with HG was

significantly reduced (Fig. 5b), which was consistent with the conclusion drawn by our bioinformatics analysis.

Sequentially, the expression levels of EMT-related proteins (nephrin, α -SMA and vimentin) and apoptotic protein Bim were also detected via WB method (Fig. 6). According to the existing literature, α -SMA and vimentin are two cytoskeletal proteins, in which α -SMA is a marker of smooth muscle cells, while vimentin is an intermediate product of renal tubular epithelial cells during their transformation into myofibroblasts [19, 20]. And nephrin is specifically expressed in the podocyte hiatus membrane, the loss of which could destroy the integrity of the glomerular filtration barrier, further incur massive proteinuria [21]. Protein Bim, as one of the Bcl-2 family proteins, could promote cell apoptosis. In this experiments, we discovered the decrease of *BTG2* stimulated by HG significantly corresponded to the decrease of nephrin and the increase of α -SMA, vimentin and Bim. And overexpression of *BTG2* could partially reverse this phenomenon, suggesting that *BTG2* could inhibit the EMT and reduce the podocytes apoptosis. Cell scratch assay is a method for cell migration assessment. The target cells were placed in a culture medium with scratches and then observed how the cells repaired these injuries and migrated to adjacent areas. Through

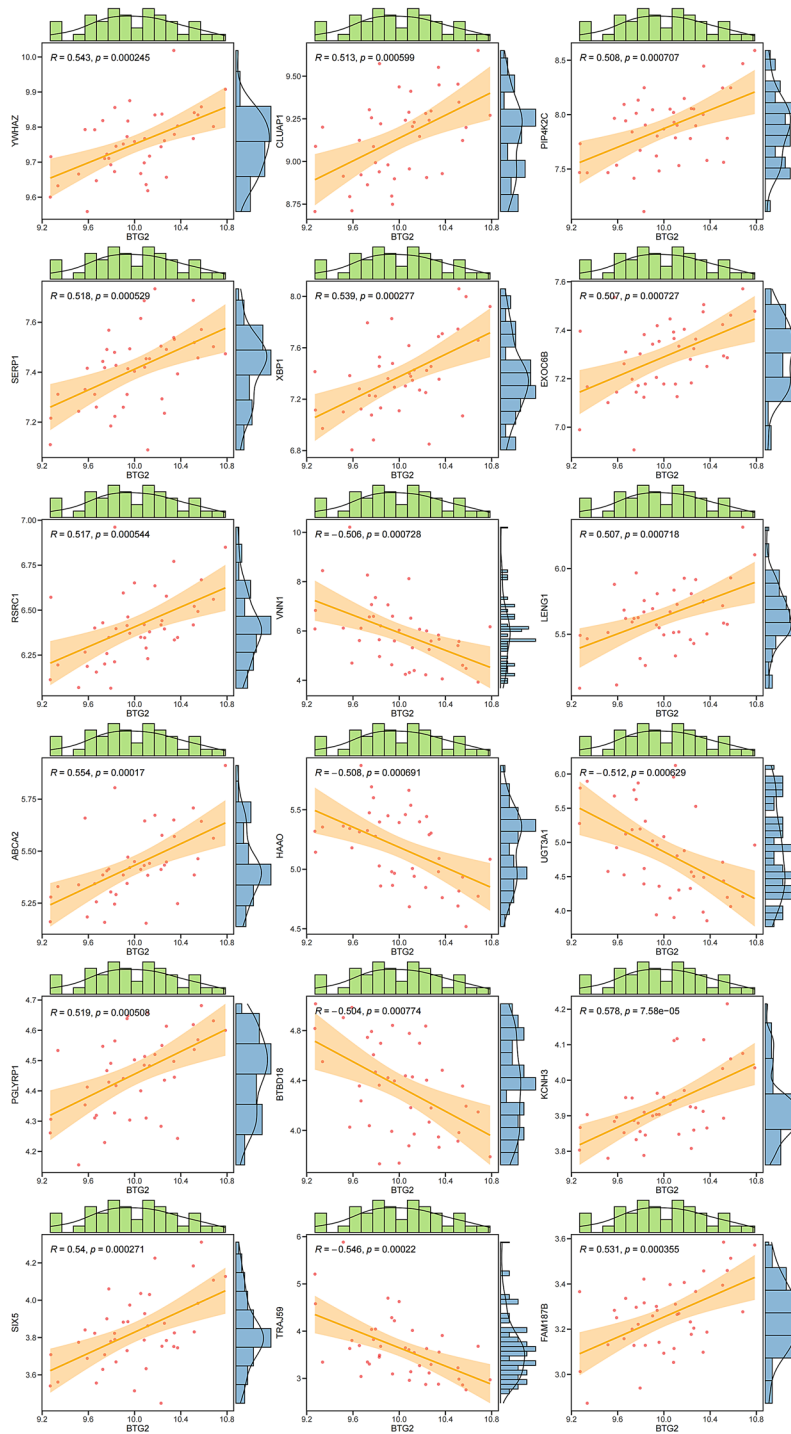


Fig. 2 Pearson correlation analysis for BTG2 from DKD samples correlation R value stands for correlation coefficient, while positive values represent positive correlation and negative values represent negative correlation. The greater the absolute value of R, the stronger the correlation. Coefficient > 0.5 or < -0.5, P < 0.05

statistical analysis of the percentage of Cell scratch distance between scratches, it is possible to visualize cells migration ability. The results showed that compared with normal podocytes, the migration ability of podocytes was significantly improved after inhibiting *BTG2* or exposure

to HG (Fig. 7), while gene overexpression could retard the migration, suggesting a control of *BTG2* to EMT in a way. Notably, EMT refers to a stronger migration ability. Flow cytometry was also conducted to probe the influence of *BTG2* on podocyte apoptosis (Fig. 8). We employed flow

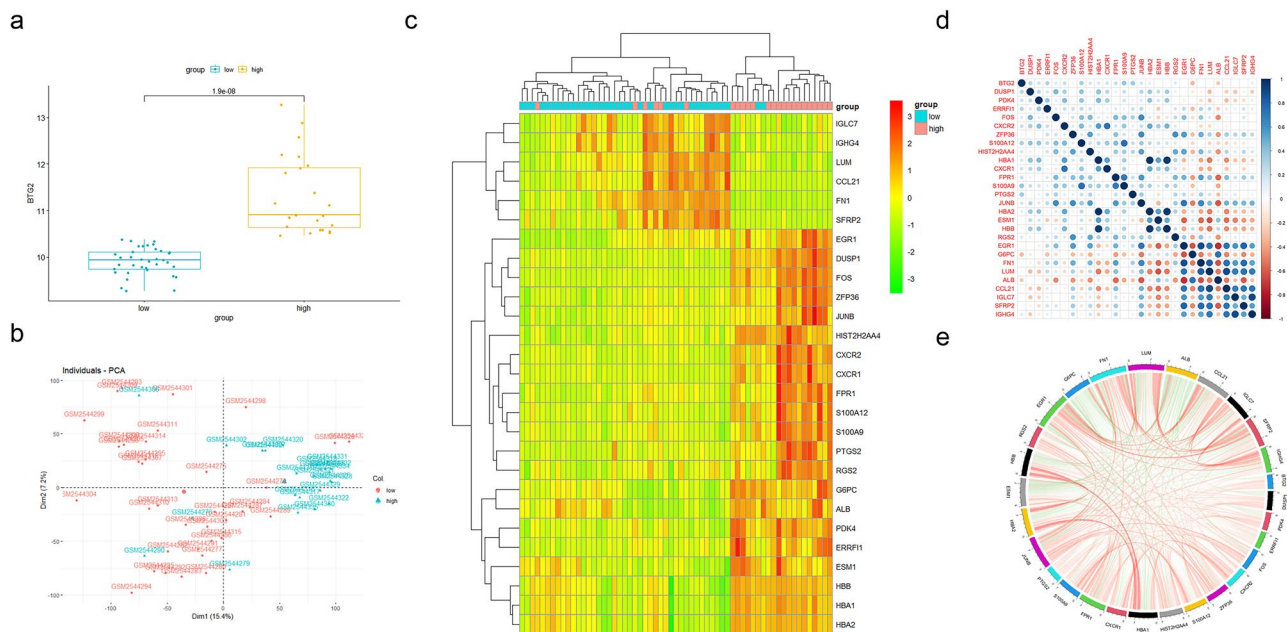


Fig. 3 DEGs selected by *BTG2* expression level (a) Comparison of *BTG2* differential expression in DKD patients. Dividing DKD patients into *BTG2* higher and lower expression groups, higher *BTG2* group has significantly higher *BTG2* expression level than the lower. (b) PCA of *BTG2* differential expression in DKD dataset. Clustered samples indicated little difference between the samples. (c) Heatmap of DEGs. Demonstrated the synergistic relationship between DEGs and *BTG2* expression. (d) Correlation heatmap between *BTG2* and the coding genes. (e) Circos plot between *BTG2* and the coding genes. Log₂ FC > 1.5 or < -1.5, adjust P value < 0.05

cytometer measuring podocytes fluorescence intensity and staining characteristics treated with HG and further analyzed statistically. We found when the expression of *BTG2* decreased, the percentage of apoptotic cells significantly increased, and this manifestation was also alleviated by *BTG2* overexpression.

Finally, we examined the effects of *BTG2* expression on mTORC1 signaling pathway and autophagy using WB (Fig. 9). It was found that compared with the normal, exposure to HG gave rise to increases in pRPS6KB1/RPS6KB1 ratio and mTOR/TOR ratio, while a decrease in autophagy protein LC3 II/LC3 I ratio was detected. And these were partially reversed when *BTG2* was overexpressed, suggesting *BTG2*'s possible promotion of autophagy via mTORC1 signaling pathway inhibition.

Discussion

Diabetic Kidney Disease (DKD) is rapidly becoming a leading cause of Chronic Kidney Disease (CKD) and its associated morbidity and mortality [22]. Extensive research has established connections between DKD and other conditions, such as periodontitis [23–25]. Notably, significant differences in the oral flora of periodontitis patients have been observed between DKD patients and diabetics without DKD [26]. The influence of oral and periodontal microflora on systemic diseases extends beyond local inflammatory reactions, involving the dissemination of oral microbial virulence through the bloodstream, oropharynx, and respiratory tract [27]. This

increasing prevalence of DKD necessitates deeper investigation into its association with periodontitis.

With the advancement of bioinformatics, we supplied this method to probe the interaction between DKD and periodontitis. We downloaded and analyzed the gene expression data sets in GEO. The results showed that the gene *BTG2* was a common DEG of periodontitis and DKD. *BTG2* was underexpressed significantly in DKD than the normal and correlated with clinical prognostic indicators like albuminuria. When probing the possible pathway that *BTG2* affects on DKD, we firstly organized GSEA, a bioinformatics tool detecting the enrichment pathway of target gene, and the results indicated that EMT pathway as well as mTORC1 signaling pathway might involve in the way *BTG2* works between periodontitis and DKD. EMT refers to the biological process epithelial cells transformed into cells with mesenchymal phenotype, and the main characteristics are the reduction of the expression of cell adhesion molecules (such as E-cadherin), the transformation of cytoskeleton from keratin to vimentin, and the morphological characteristics of mesenchymal cells [28, 29]. About mTORC1 signaling pathway, pivotal protein mTORC1 is a vital regulator of EMT. In the way to EMT, mTORC1 is conducive to cell enlargement, protein synthesis, motility and invasion, while mTORC2 is necessary for epithelial to mesenchymal phenotype transition [30–32]. According to the literature published, EMT is a pivotal contributor for renal fibrosis, since about 30% of fibroblasts are

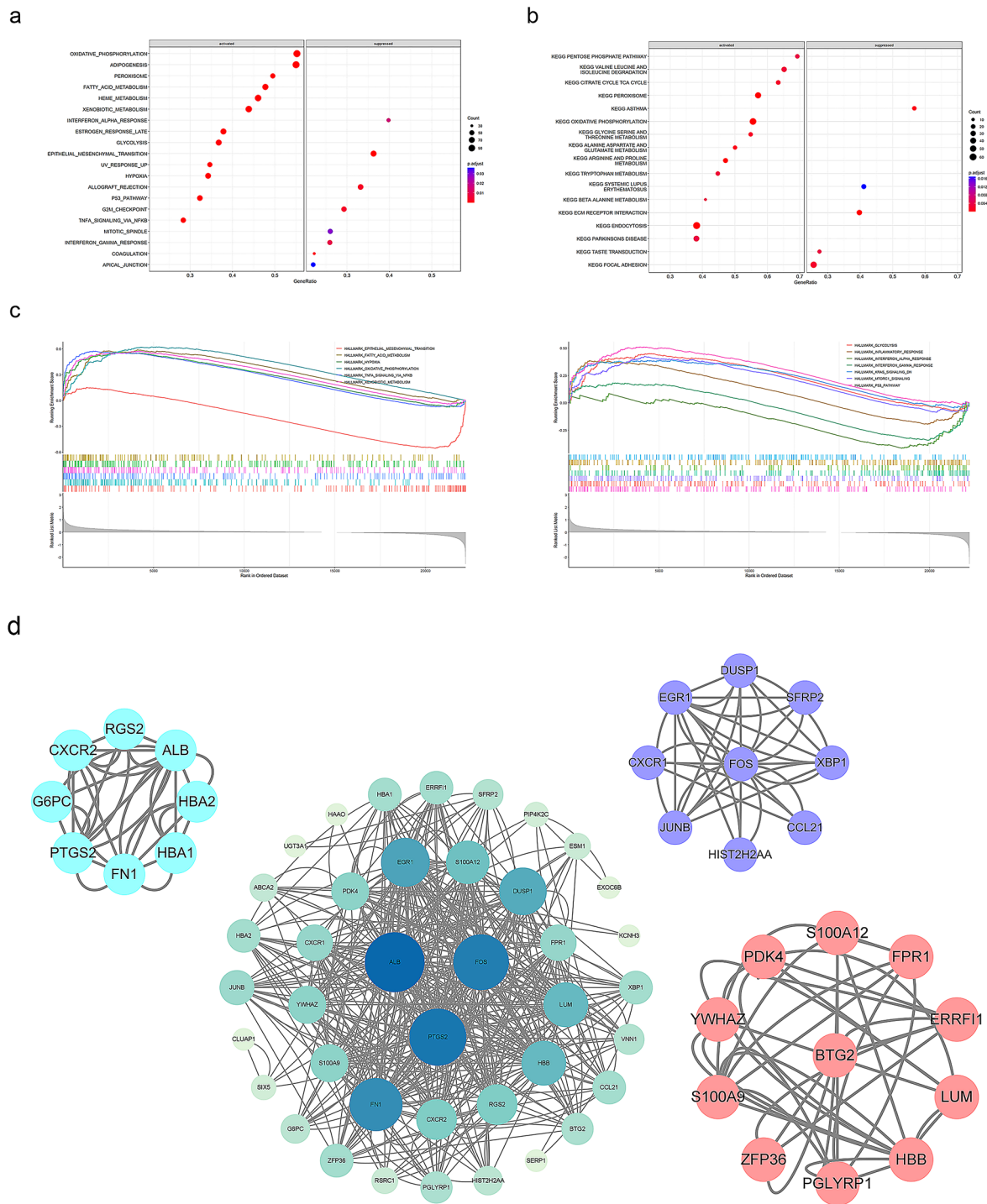


Fig. 4 DEGs functional analysis: a: Bubble diagram based on gene sets *h.all.v7.1.symbols.gmt*. b: Bubble diagram based on gene sets *c2.cp.kegg.v7.1.symbols.gmt*. Count represents bubble size and color represents adjusted *P*. GeneRatio = count / number of annotated gene. c: GSEA of BTG2 enrichment pathway. Each bar represents a gene, and the vertical coordinates represented the enrichment scores of the genes. Positive scores are regarded as gene activation, and negative scores are regarded as gene inhibition. d: PPI network constructed by cytoscape software. Parameter setting: Degree Cutoff: 2, Node Score Cutoff: 0.2, K-Core: 2, Max.Depth: 100. Cluster 1: 4.571 points, Cluster 2: 4.25 points, cluster 3: 3.6 points

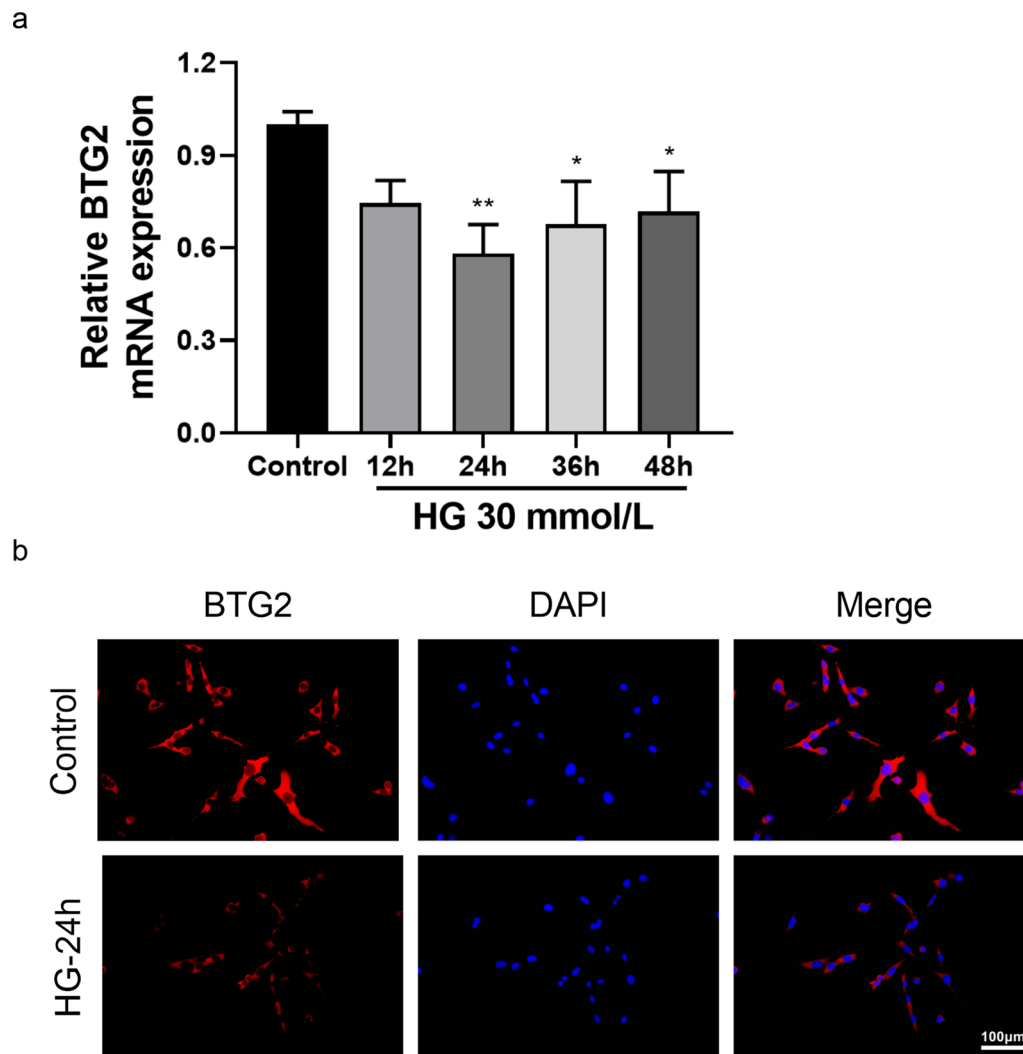


Fig. 5 BTG2 optimal exposure time determination and expression change to HG **a**:the BTG2 mRNA expression level under different HG (30mmol/L) exposure time detected by aPCR. When exposed to HG for 24 h, *BTG2* has the lowest expression level. **b**: BTG2 expression change when exposed to HG in immunofluorescence assay. *, $P < 0.05$; **, $P < 0.01$

derived from the tubular epithelial cells via EMT [33, 34]. Hyperglycaemia can induce EMT, and upon EMT, or other stimuli induced by high glucose, podocytes can change their epithelial cells phenotype to mesenchymal cells [35]. Finally, EMT of tubular epithelial cells and glomerular podocytes would incur tubulointerstitial fibrosis and glomerulosclerosis, which indicate a poor long-term outcomes [36].

Our study observed the changes of EMT-related and mTORC1 signaling pathway proteins in podocytes when the *BTG2* expression was reduced under the HG condition. We discovered that, compared with the normal, proteins had a significant increase, representing a EMT and mTORC1 signaling pathway promotion. Cell scratch assay showed that compared with the control, reducing the *BTG2* expression in normal podocytes could promote cell motility, when this was more apparent in the

group exposed to HG. As we all know, the remarkable feature of EMT is a stronger migration ability. Thus the assay reflected the inhibition of *BTG2* to EMT from the side. Correspondingly, up-regulation *BTG2* again in HG group restraining the cell motility corroborated this supposition. This showed that *BTG2* could inhibit EMT through mTORC1 pathway.

Considering decreased mTORC1 activity can induce autophagy, we also detected changes of autophagy protein following the *BTG2* expression level. Autophagy is a significant mechanism for cellular homeostasis maintenance through potentially toxic components removal and degraded substances recycle [37]. Autophagy mediate EMT, and loss of autophagy will dramatically promote the EMT [38]. Aberrant autophagy is the main character of CKD and autophagy inducement can protect kidney from damage [39, 40]. In this study, we found

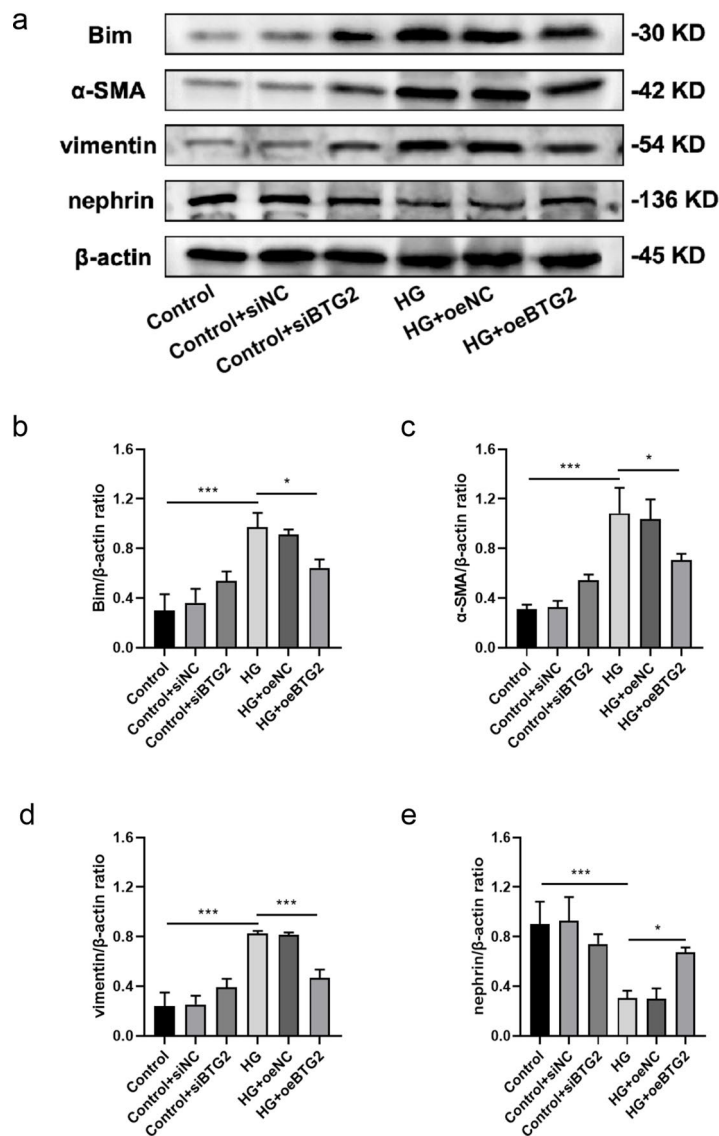


Fig. 6 The relationship between BTG2 and EMT and apoptotic related proteins **a**: Western blot between BTG2 and nephrin, α-SMA, vimentin, Bim. **b**: Histogram of BTG2's relation with Bim. Compared to the control, exposed to HG had a higher Bim/β-actin ratio. Compared to HG exposure, over-expressing *BTG2* under HG had a lower Bim/β-actin ratio. **c**: Histogram of BTG2's relation with α-SMA. Compared to the control, exposed to HG had a higher α-SMA/β-actin ratio. Compared to HG exposure, over-expressing *BTG2* under HG had a lower α-SMA/β-actin ratio. **d**: Histogram of BTG2's relation with vimentin. Compared to the control, exposed to HG had a higher vimentin/β-actin ratio. Compared to HG exposure, over-expressing *BTG2* under HG had a lower vimentin/β-actin ratio. **e**: Histogram of BTG2's relation with nephrin. Compared to the control, exposed to HG had a lower nephrin/β-actin ratio. Compared to HG exposure, over-expressing *BTG2* under HG had a higher α-SMA/β-actin ratio. Internal reference control: β-actin; NC: negative control; *, $P < 0.05$; ***, $P < 0.001$

when *BTG2* was inhibited, autophagy protein had a significant decrease while overexpression of *BTG2* could reverse this tendency. So we have enough reason to believe that *BTG2* could inhibit mTORC1 signaling pathway, enhance autophagy, therefore restraining EMT.

Although the related of *BTG2* in this pathway have not yet been further confirmed, but the PPI network in this study conducted demonstrated that *BTG2* was relevant to the genes *S100A9* and *S100A12*. Both belong to the S100 protein family, *S100A9* and *S100A12* are linked with

systematic inflammation while sustained inflammation represents the deterioration of renal interstitial fibrosis [41–44]. Targeting the *S100A9* signaling with inhibitors could decrease inflammation, ameliorate kidney injury, improve renal function and improved long-term outcomes such as mortality reduction with decreased renal fibrosis [45]. *S100A12* was declared to show expression in renal endothelial cells [42] and was deemed as a predictor of increased CKD mortality risk in a manner that was independent of the soluble advanced glycation

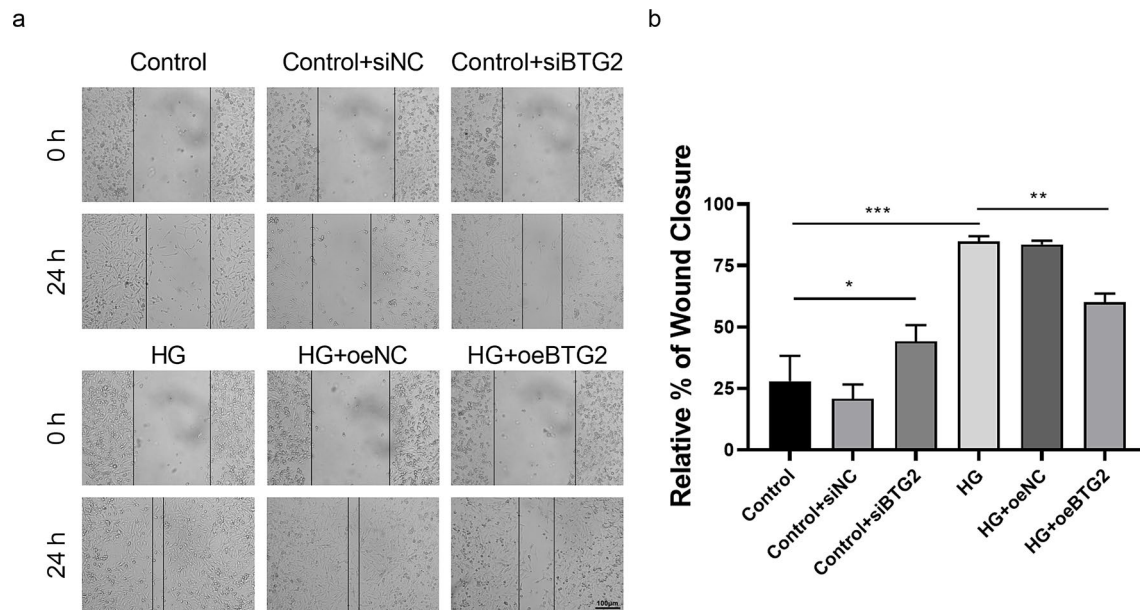


Fig. 7 The relationship between *BTG2* expression and podocytes migration ability **a**. Wound healing assay of *BTG2* expression to cell migration ability. The wound closure rates were observed to compare cell migration ability under the condition of *BTG2* underexpression and overexpression. **b**: Relative % of wound closure. Compared to the control, under-expressing *BTG2* and exposed to HG had better wound closure. Compared to HG exposure, over-expressing *BTG2* under HG had worse wound closure. NC: negative control; *, $P < 0.05$; ***, $P < 0.001$

end-products receptor [46]. Combined with these published articles, we speculate that *BTG2* may have a correlation with *S100A9* and *S100A12* in the way it actions on the EMT pathway.

Interestingly, our cell experiments also revealed *BTG2*'s role in reducing podocyte apoptosis. This finding is intriguing, given the traditional view of EMT as being anti-apoptotic. It has been demonstrated that in many cells including renal cells, EMT and apoptosis concomitantly occurs [47–49]. Therefore, we hold the opinion that *BTG2* might independently influence apoptosis, separate from its effects on EMT, which should be warranted with further investigation.

Considering *BTG2* as the target gene that affecting DKD, regulating the upstream factors or pathways that lead to the *BTG2* decrease to increase *BTG2* expression in DKD, further affecting subsequent reactions including EMT and autophagy, could finally influence the occurrence and development of DKD. However, due to time and resource limitations, we have not proved the potential mechanism of how *BTG2* affect apoptosis yet, and we did not further detect the detailed proteins or molecules involved in the EMT pathway *BTG2* located, which would restrict the clinical development and application of drug targeted therapy. We will conduct further explorations in the future to examine the essential role of *BTG2* and detailed pathway *BTG2* located between periodontitis and DKD.

Conclusion

In conclusion, our study used both bioinformatic analysis and cellular functional assays to testify that *BTG2* emerges as a key gene in the interaction between DKD and periodontitis, potentially up-regulating autophagy by inhibiting the mTORC1 signaling pathway, thereby inhibiting EMT.

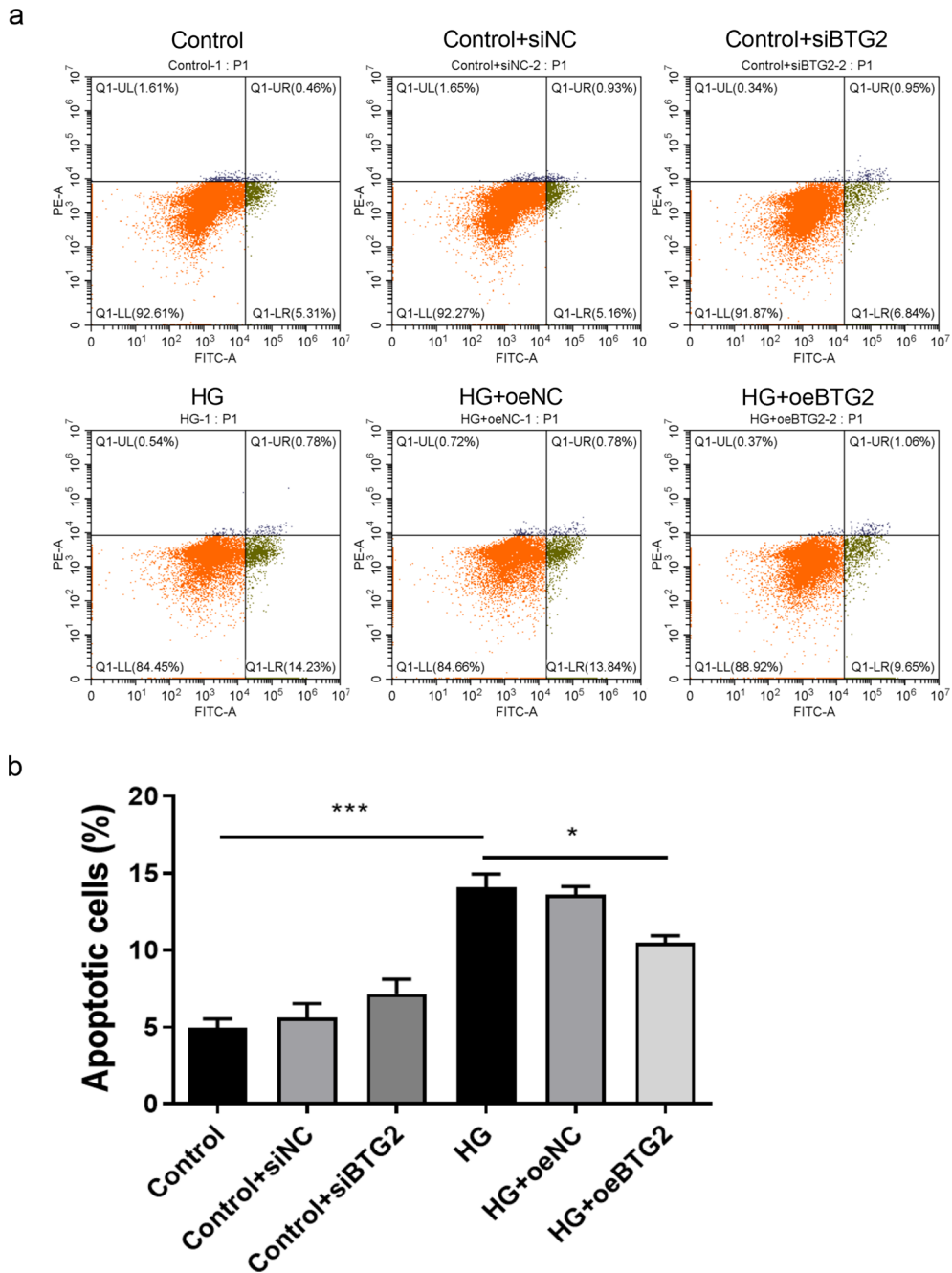


Fig. 8 The relationship between BTG2 expression and podocyte apoptosis **a**: Flow apoptosis assay of BTG2 to cell apoptosis. **b**: Apoptosis cells (%) with BTG2 expression change. Compared to the control, exposed to HG had much more apoptotic cells. Compared to HG exposure, over-expressing *BTG2* under HG had less apoptotic cells. NC, negative control; si, under-express; oe, over-express. *, $P < 0.05$; ***, $P < 0.001$

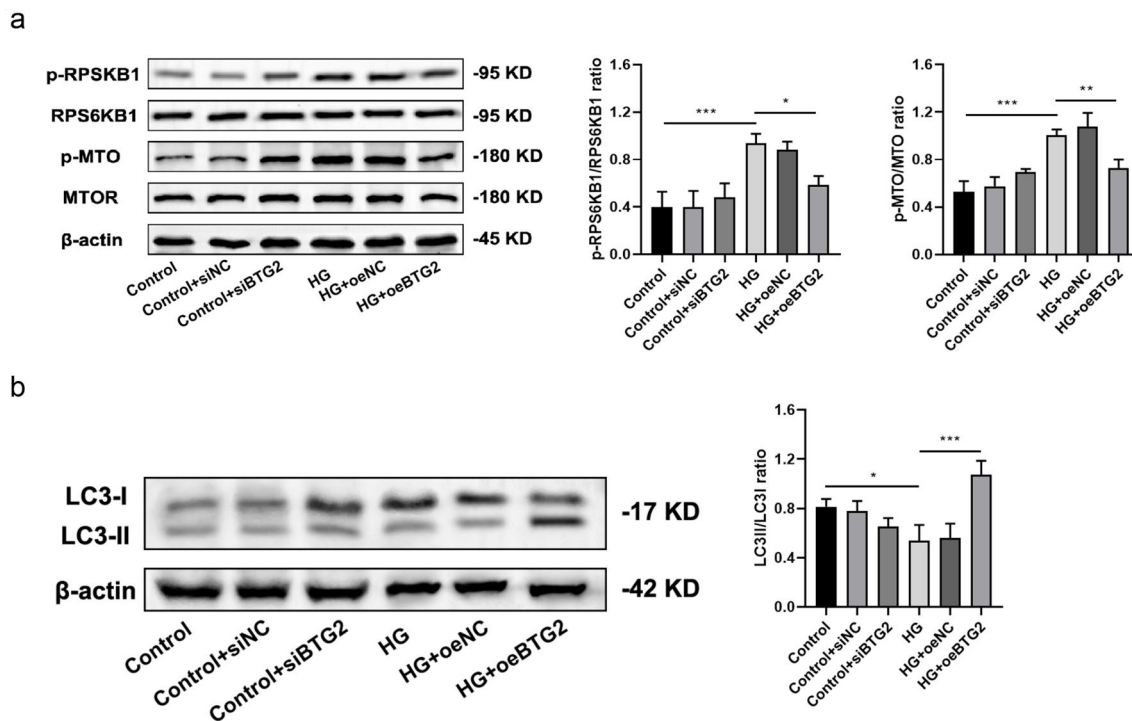


Fig. 9 The relationship between BTG2 and mTORC1 signaling pathway and autophagy related proteins **a**: Western blot of BTG2 to RPS6KB1 and mTORC1. Compared to the control, exposed to HG had higher p-RPS6KB1/RPS6KB1 and p-MTORC1/MTORC1 ratios. Compared to HG exposure, over-expressing BTG2 under HG had lower p-RPS6KB1/RPS6KB1 and p-MTORC1/MTORC1 ratios. **b**: Western blot of BTG2 to autophagy protein LC3. Compared to the control, exposed to HG had a lower LC3II/LC3I ratio. Compared to HG exposure, over-expressing BTG2 under HG had a higher LC3II/LC3I ratio. Internal reference control: β -actin; NC: negative control; * $P < 0.05$; ** $P < 0.01$; *** $P < 0.001$

Abbreviations

CKD	Chronic Kidney Disease
DEGs	Differentially Expressed Genes
DKD	Diabetic Kidney Disease
EMT	Epithelial-To-Mesenchymal Transition
GEO	Gene Expression Omnibus
GSEA	Gene Set Enrichment Analysis
HG	High Glucose
MCODE	Molecular Complex Detection
mTOR	Mammalian Target of Rapamycin
PBS	Phosphate Buffered Saline
PPI	Protein-Protein Interaction
qPCR	Quantitative Polymerase Chain Reaction
RPS6KB1	Ribosomal Protein S6 Kinase B1
WB	Western Blotting

Acknowledgements

Not applicable.

Author contributions

Binhui Pan and Yangyang Teng have contributed equally to this work. BP and YT conceived this research, performed the data analysis and experimental verification, and wrote the manuscript. RW and DC performed bioinformatics analyses and assisted with analyzing other data. HC helped to revise the manuscript. All authors have read and approved the final manuscript.

Funding

This work was supported by Wenzhou Science and Technology Bureau [Y2023365].

Data availability

The full uncropped Gels and Blots images supporting the conclusions of this article and method details are included in the supplementary file. Periodontitis and DKD data were deposited into the Gene Expression Omnibus database under accession number GSE16134, GSE10334 and

GSE96804, which are available at the following URL: <https://www.ncbi.nlm.nih.gov/geo/query/acc.cgi?acc=GSE16134>, <https://www.ncbi.nlm.nih.gov/geo/query/acc.cgi?acc=GSE10334>, <https://www.ncbi.nlm.nih.gov/geo/query/acc.cgi?acc=GSE96804>.

Ethics approval

Human data were downloaded from public database and there are no relevant data about human participants, their data or biological material that need ethics approval. Rats cell lines were purchased from life science company. Cell Line: MPC-5 mouse cell line RRID: iCell-m081.

Consent for publication

Not applicable.

Competing interests

The authors declare no competing interests.

Received: 2 April 2024 / Accepted: 16 May 2024

Published online: 03 June 2024

References

- Alicic RZ, Rooney MT, Tuttle KR. Diabetic kidney disease: challenges, Progress, and possibilities. *Clin J Am Soc Nephrol.* 2017;12(12):2032–45.
- Global regional, national burden of chronic kidney disease. 1990–2017: a systematic analysis for the global burden of Disease Study 2017. *Lancet.* 2020;395(10225):709–33.
- Krutyholowa A, Strzelec K, Dziedzic A, et al. Host and bacterial factors linking periodontitis and rheumatoid arthritis. *Front Immunol.* 2022;13:980805.
- Gupta K, Kaur N, Kaur G. The plausible relationship between periodontitis and Glaucoma. *Cureus.* 2022;14(7):e27440.
- Chen L, Nini W, Jinmei Z, Jingmei Y. Implications of sleep disorders for periodontitis. *Sleep Breath.* 2022.

6. Wadia R. Periodontitis and systemic inflammation. *Br Dent J.* 2022;233(6):494.
7. Wadia R. Periodontal Disease & lung cancer. *Br Dent J.* 2020;229(2):125.
8. Shultis WA, Weil EJ, Looker HC, et al. Effect of periodontitis on overt nephropathy and end-stage renal disease in type 2 diabetes. *Diabetes Care.* 2007;30(2):306–11.
9. Kajiwara K, Sawa Y, Fujita T, Tamaoki S. Immunohistochemical study for the expression of leukocyte adhesion molecules, and FGF23 and ACE2 in P. Gingivalis LPS-induced diabetic nephropathy. *BMC Nephrol.* 2021;22(1):3.
10. Sawa Y, Takata S, Hatakeyama Y, Ishikawa H, Tsuruga E. Expression of toll-like receptor 2 in glomerular endothelial cells and promotion of diabetic nephropathy by Porphyromonas gingivalis lipopolysaccharide. *PLoS ONE.* 2014;9(5):e97165.
11. Chen Y, Wang C, Wu J, Li L. BTG/Tob family members Tob1 and Tob2 inhibit proliferation of mouse embryonic stem cells via Id3 mRNA degradation. *Biochem Biophys Res Commun.* 2015;462(3):208–14.
12. Velayutham N, Calderon MU, Alfieri CM, et al. Btg1 and Btg2 regulate neonatal cardiomyocyte cell cycle arrest. *J Mol Cell Cardiol.* 2023;179:30–41.
13. Song J, Xu F, An L, et al. BTG2 suppresses the growth and metastasis of cervical squamous cell carcinoma. *Pathol Res Pract.* 2023;247:154577.
14. Yang W, Wei C, Cheng J, et al. BTG2 and SerpinB5, a novel gene pair to evaluate the prognosis of lung adenocarcinoma. *Front Immunol.* 2023;14:1098700.
15. Qi F, Liu W, Tan B, et al. BTG2 suppresses renal cell carcinoma progression through N6-methyladenosine. *Front Oncol.* 2022;12:1049928.
16. Guo D, Hong L, Ji H, et al. The mutation of BTG2 gene predicts a poor outcome in primary testicular diffuse large B-Cell lymphoma. *J Inflamm Res.* 2022;15:1757–69.
17. Zhang L, Wang X. Lowly expressed LNC01136 fails to aid HIF-1 α to induce BTG2 expression resulting in increased proliferation of retinal microvascular endothelial cells. *Microvasc Res.* 2022;141:104315.
18. Hoffman MJ, Takizawa A, Jensen ES, et al. Btg2 mutation induces renal injury and impairs blood pressure control in female rats. *Physiol Genomics.* 2022;54(7):231–41.
19. Hay ED. An overview of epithelio-mesenchymal transformation. *Acta Anat (Basel).* 1995;154(1):8–20.
20. Hewitson TD, Wu HL, Becker GJ. Interstitial myofibroblasts in experimental renal infection and scarring. *Am J Nephrol.* 1995;15(5):411–7.
21. Ruotsalainen V, Patrakka J, Tissari P, et al. Role of nephrin in cell junction formation in human nephrogenesis. *Am J Pathol.* 2000;157(6):1905–16.
22. Rayego-Mateos S, Rodrigues-Diez RR, Fernandez-Fernandez B, et al. Targeting inflammation to treat diabetic kidney disease: the road to 2030. *Kidney Int.* 2023;103(2):282–96.
23. Kajiwara K, Sawa Y, Fujita T, Tamaoki S. Immunohistochemical study for the expression of leukocyte adhesion molecules, and FGF23 and ACE2 in P. Gingivalis LPS-induced diabetic nephropathy. 2021. 22(1): 3.
24. Sawa Y, Takata S, Hatakeyama Y, Ishikawa H, Tsuruga E. Expression of toll-like receptor 2 in glomerular endothelial cells and promotion of diabetic nephropathy by Porphyromonas gingivalis lipopolysaccharide. 2014. 9(5): e97165.
25. Wu HQ, Wei X, Yao JY et al. Association between retinopathy, nephropathy, and periodontitis in type 2 diabetic patients: a Meta-analysis. 2021. 14(1): 141–7.
26. Zhang D, Liu W, Peng L, et al. Difference in oral microbial composition between chronic periodontitis patients with and without diabetic nephropathy. *BMC Oral Health.* 2022;22(1):12.
27. Amato A. Periodontitis and Cancer: beyond the boundaries of oral cavity. *Cancers (Basel).* 2023. 15(6): 1736.
28. Liu Y. New insights into epithelial-mesenchymal transition in kidney fibrosis. *J Am Soc Nephrol.* 2010;21(2):212–22.
29. Kriz W, Kaissling B, Le Hir M. Epithelial-mesenchymal transition (EMT) in kidney fibrosis: fact or fantasy. *J Clin Invest.* 2011;121(2):468–74.
30. Dongre A, Weinberg RA. New insights into the mechanisms of epithelial-mesenchymal transition and implications for cancer. *Nat Rev Mol Cell Biol.* 2019;20(2):69–84.
31. Lamouille S, Derynck R. Cell size and invasion in TGF-beta-induced epithelial to mesenchymal transition is regulated by activation of the mTOR pathway. *J Cell Biol.* 2007;178(3):437–51.
32. Lamouille S, Connolly E, Smyth JW, Akhurst RJ, Derynck R. TGF- β -induced activation of mTOR complex 2 drives epithelial-mesenchymal transition and cell invasion. *J Cell Sci.* 2012;125(Pt 5):1259–73.
33. Zhang N, Gao Y, Zou D et al. Effects of Chinese Medicine Tong xinluo on Diabetic Nephropathy via Inhibiting TGF- β 1-Induced Epithelial-to-Mesenchymal Transition. *Evid Based Complement Alternat Med.* 2014. 2014: 123497.
34. Tang G, Li S, Zhang C, Chen H, Wang N, Feng Y. Clinical efficacies, underlying mechanisms and molecular targets of Chinese medicines for diabetic nephropathy treatment and management. *Acta Pharm Sin B.* 2021;11(9):2749–67.
35. Zhang M, Liu M, Xiong M, Gong J, Tan X. Schisandra chinensis fruit extract attenuates albuminuria and protects podocyte integrity in a mouse model of streptozotocin-induced diabetic nephropathy. *J Ethnopharmacol.* 2012;141(1):111–8.
36. Hadjpech S, Thongboonkerd V. Epithelial-mesenchymal plasticity in kidney fibrosis. *Genesis.* 2023: e23529.
37. He L, Wei Q, Liu J, et al. AKI on CKD: heightened injury, suppressed repair, and the underlying mechanisms. *Kidney Int.* 2017;92(5):1071–83.
38. Li J, Yang B, Zhou Q, et al. Autophagy promotes hepatocellular carcinoma cell invasion through activation of epithelial-mesenchymal transition. *Carcinogenesis.* 2013;34(6):1343–51.
39. Periyasamy-Thandavan S, Jiang M, Wei Q, Smith R, Yin XM, Dong Z. Autophagy is cytoprotective during cisplatin injury of renal proximal tubular cells. *Kidney Int.* 2008;74(5):631–40.
40. Kaushal GP, Shah SV. Autophagy in acute kidney injury. *Kidney Int.* 2016;89(4):779–91.
41. Vogl T, Gharibyan AL, Morozova-Roche LA. Pro-inflammatory S100A8 and S100A9 proteins: self-assembly into multifunctional native and amyloid complexes. *Int J Mol Sci.* 2012;13(3):2893–917.
42. Donato R, Cannon BR, Sorci G, et al. Functions of S100 proteins. *Curr Mol Med.* 2016;13(1):24–57.
43. Lovisa S, Zeisberg M, Kalluri R. Partial epithelial-to-mesenchymal transition and other New mechanisms of kidney fibrosis. *Trends Endocrinol Metab.* 2016;27(10):681–95.
44. Austermann J, Spiekermann C, Roth J. S100 proteins in rheumatic diseases. *Nat Rev Rheumatol.* 2018;14(9):528–41.
45. Yao W, Chen Y, Li Z, et al. Single cell RNA sequencing identifies a unique inflammatory macrophage subset as a Druggable Target for alleviating Acute kidney Injury. *Adv Sci (Weinh).* 2022;9(12):e2103675.
46. Isoyama N, Leurs P, Qureshi AR, et al. Plasma S100A12 and soluble receptor of advanced glycation end product levels and mortality in chronic kidney disease stage 5 patients. *Nephrol Dial Transpl.* 2015;30(1):84–91.
47. Docherty NG, O'Sullivan OE, Healy DA, et al. TGF-beta1-induced EMT can occur independently of its proapoptotic effects and is aided by EGF receptor activation. *Am J Physiol Ren Physiol.* 2006;290(5):F1202–12.
48. Wang HJ, Zhu J, Zheng GY. Role of glutathione and other antioxidants in the inhibition of apoptosis and mesenchymal transition in rabbit lens epithelial cells. *Genet Mol Res.* 2014;13(3):7149–56.
49. Franco DL, Mainez J, Vega S, et al. Snail1 suppresses TGF-beta-induced apoptosis and is sufficient to trigger EMT in hepatocytes. *J Cell Sci.* 2010;123(Pt 20):3467–77.

Publisher's Note

Springer Nature remains neutral with regard to jurisdictional claims in published maps and institutional affiliations.